

## Cleavage of Various Peptides with Pitrilysin from *Escherichia coli*: Kinetic Analyses Using $\beta$ -Endorphin and Its Derivatives

Joel CORNISTA,<sup>1</sup> Satoshi IKEUCHI,<sup>1</sup> Mitsuru HARUKI,<sup>1,\*</sup> Atsuko KOHARA,<sup>2</sup> Kazufumi TAKANO,<sup>1,3</sup> Masaaki MORIKAWA,<sup>1,\*\*</sup> and Shigenori KANAYA<sup>1,†</sup>

<sup>1</sup>Department of Material and Life Science, Graduate School of Engineering, Osaka University, 2-1 Yamadaoka, Suita, Osaka 565-0871, Japan

<sup>2</sup>Protein Engineering Research Institute, 6-2-3 Furuedai, Suita, Osaka 565-0874, Japan

<sup>3</sup>PRESTO, JST, 2-1 Yamadaoka, Suita, Osaka 565-0871, Japan

Received May 26, 2004; Accepted July 16, 2004

**Pitrilysin from *Escherichia coli* was overproduced, purified, and analyzed for enzymatic activity using 14 peptides as a substrate. Pitrilysin cleaved all the peptides, except for two of the smallest, at a limited number of sites, but showed little amino acid specificity. It cleaved  $\beta$ -endorphin ( $\beta$ -EP) most effectively, with a  $K_m$  value of  $0.36 \mu\text{M}$  and a  $k_{\text{cat}}$  value of  $750 \text{ min}^{-1}$ .  $\beta$ -EP consists of 31 residues and was predominantly cleaved by the enzyme at Lys<sup>19</sup>–Asn<sup>20</sup>. Kinetic analyses using a series of  $\beta$ -EP derivatives with N and/or C-terminal truncations and with amino acid substitutions revealed that three hydrophobic residues (Leu<sup>14</sup>, Val<sup>15</sup>, and Leu<sup>17</sup>) and the region 22–26 in  $\beta$ -EP are responsible for high-affinity recognition by the enzyme. These two regions are located on the N- and C-terminal sides of the cleavage site in  $\beta$ -EP, suggesting that the substrate binding pocket of pitrilysin spans its catalytic site.**

**Key words:** insulysin; kinetic analysis; metallopeptidase; pitrilysin; substrate specificity

*Escherichia coli* pitrilysin (EC 3.4.24.55), which has also been designated as protease III or Pi, is a metallopeptidase that requires divalent cations, such as Zn<sup>2+</sup>, Co<sup>2+</sup>, Mn<sup>2+</sup>, and Ca<sup>2+</sup>, for activity.<sup>1,2</sup> It is a periplasmic enzyme<sup>3</sup> and acts in monomeric form.<sup>2,4</sup> The *ptr* gene encoding this enzyme is located in the chromosome between the *recB* and *recC* genes, which encode subunits of endonuclease V.<sup>5</sup> The physiological role of pitrilysin is not known, because gene disruption studies have indicated that this enzyme is not essential for normal cell growth.<sup>6,7</sup> The nucleotide sequence of the *ptr* gene reveals that pitrilysin is synthesized in a

precursor form, which contains a typical signal peptide with 23 amino acid residues at the N-terminus.<sup>8</sup> This signal peptide is expected to be removed upon secretion into the periplasmic space to produce a mature form of the enzyme that is composed of 939 amino acid residues with a molecular mass of 105,108 Da.

Pitrilysin shows amino acid sequence identities of 21–29% with mammalian insulysins (insulin-degrading enzymes, IDEs),<sup>9–11</sup> rat N-arginine dibasic convertase,<sup>12</sup> zinc metalloprotease from plants,<sup>13</sup> human metalloprotease 1 (MP1),<sup>14</sup> chloroplast processing enzyme (CPE),<sup>15</sup> falcilysin from malaria parasite,<sup>16</sup> and yeast AXL1 protease.<sup>17</sup> All of these enzymes, which are members of the insulysin family or metallopeptidase clan ME family M16 according to Rawlings,<sup>18</sup> contain the active-site sequence motif HXXEH(X)<sub>n</sub>E, where n is 76 in most cases and X could be any amino acid. The initial five-residue sequence motif (HXXEH) is an inversion of the active-site motif (HEXXH) found in other metallopeptidases, such as thermolysin and aminopeptidases.<sup>19</sup> Site-directed mutagenesis studies have revealed that two histidine residues and the second glutamate within this sequence motif (His<sup>88</sup>, His<sup>92</sup>, and Glu<sup>169</sup> for pitrilysin and His<sup>108</sup>, His<sup>112</sup>, and Glu<sup>189</sup> for human insulysin) are required for metal binding, while the first glutamate (Glu<sup>91</sup> for pitrilysin and Glu<sup>111</sup> for human insulysin) is required for catalysis.<sup>20–24</sup>

Among various metalloproteases, research interest in human insulysin has emerged because of its ability to cleave a number of biologically important peptides, such as insulin and amyloid  $\beta$ -protein, implicated in the Alzheimer's disease.<sup>25</sup> Because of the potential physiological and biomedical significance of this enzyme,

† To whom correspondence should be addressed. Fax: +81-6-6879-7938; E-mail: kanaya@mls.eng.osaka-u.ac.jp

\* Present address: Department of Materials Chemistry and Engineering, College of Engineering, Nihon University, Tamura-machi, Koriyama, Fukushima 963-8642, Japan

\*\* Present address: Laboratory of Environmental Molecular Biology, Graduate School of Environmental Earth Science, Hokkaido University, Sapporo 060-0810, Japan

Abbreviations:  $\beta$ -EP,  $\beta$ -endorphin; insulin B, oxidized insulin B chain; ANP, atrial natriuretic peptide; VIP, vasoactive intestinal peptide; ACTH, adrenocorticotropic hormone;  $\beta$ -amyloid, amyloid  $\beta$ -protein fragment 1-40; IGF II, insulin-like growth factor II; CD, circular dichroism

studies of its homologues such as pitrilysin, have recently attracted enormous attention.

The substrate recognition mechanism of insulysin family proteins remains to be elucidated, because the crystal structure is not available for any member of this family. Comprehensive and extensive studies on the substrate and cleavage-site specificities of pitrilysin, as well as its kinetic properties, should provide valuable information. Pitrilysin has been reported specifically to cleave small polypeptides with molecular masses between 1,000 and 7,000 Da.<sup>1,2)</sup> However, the cleavage-sites in these peptides remain to be determined, although the oxidized insulin B chain and vasoactive intestinal peptide (VIP) have been reported to be cleaved by the enzyme, predominantly at Tyr<sup>16</sup>-Leu<sup>17</sup> and Leu<sup>13</sup>-Arg<sup>14</sup>, respectively.<sup>1,2)</sup> In addition, degradation of the peptides by pitrilysin has not so far been analyzed kinetically, although the binding affinities of insulin, oxidized insulin B chain, and glucagon have been estimated from their  $K_i$  values for degradation of a quenched-fluorescent substrate by the enzyme.<sup>1)</sup>

In this study, pitrilysin was overproduced, purified, and analyzed for proteolytic activity using various peptide substrates. These peptides were cleaved by pitrilysin at a limited number of sites with no apparent sequence similarity. Determination of the kinetic parameters for the  $\beta$ -EP derivatives with N- and/or C-terminal truncations and those with amino acid substitutions allowed us to identify the regions in  $\beta$ -EP important for high-affinity binding of pitrilysin. Based on these results, a substrate recognition mechanism of pitrilysin is discussed.

## Materials and Methods

**Materials.** Human  $\beta$ -endorphin ( $\beta$ -EP), bovine insulin, bovine insulin B chain oxidized (insulin B), human calcitonin, bovine substance P, human glucagon, human  $\alpha$ -atrial natriuretic peptide ( $\alpha$ ANP), human adrenocorticotropic hormone fragment 1-24 (ACTH), somatostatin, bradykinin, human angiotensin I, and human amyloid  $\beta$ -protein fragment 1-40 ( $\beta$ -amyloid) were obtained from Sigma-Aldrich Japan (Tokyo). Human leuromorphin was from Peninsula Laboratories (Belmont, CA, U.S.A.), while human vasoactive intestinal peptide (VIP) was from Wako Pure Chemical (Osaka, Japan). The fragments of  $\beta$ -EP,  $\beta$ -EP<sub>9-31</sub>,  $\beta$ -EP<sub>14-31</sub>,  $\beta$ -EP<sub>18-31</sub>,  $\beta$ -EP<sub>9-26</sub>, and  $\beta$ -EP<sub>9-21</sub>, and their derivatives, [A<sup>19</sup>]- $\beta$ -EP, [N<sup>19</sup>]- $\beta$ -endorphin, [S<sup>14</sup>/S<sup>15</sup>/S<sup>17</sup>]- $\beta$ -EP<sub>9-26</sub>, [S<sup>14</sup>]- $\beta$ -EP<sub>9-26</sub>, [S<sup>15</sup>]- $\beta$ -EP<sub>9-26</sub>, [S<sup>17</sup>]- $\beta$ -EP<sub>9-26</sub>, and [S<sup>22</sup>/S<sup>23</sup>]- $\beta$ -EP<sub>9-26</sub>, were synthesized by Sawady Technology (Tokyo, Japan). Restriction and modifying enzymes used in recombinant DNA technologies were from Takara Shuzo (Kyoto, Japan) and Toyobo (Kyoto, Japan).

**Cells and plasmids.** Plasmids pUC19 and pDR540 were obtained from Takara Shuzo and Amersham Biosciences (Piscataway, NJ, U.S.A.), respectively.

*E. coli* JM109 was from Toyobo. Cells were grown in Luria-Bertani (LB) medium containing 50 mg/l ampicillin.

**Plasmid construction.** The 4.2-kbp DNA fragment containing the *ptr* gene was amplified by PCR as the *Bam*HI-*Hind*III fragment and ligated into the *Bam*HI and *Hind*III sites of pUC19 to generate plasmid pUC42. In this plasmid, the *Bam*HI and *Hind*III sites are located 50-bp upstream and 1.3-kbp downstream of the *ptr* gene, respectively. The *Hind*III site in this plasmid was converted to *Sal*I site to generate pUC42S. Finally, to place the *ptr* gene under the control of the *tac* promoter, the 400-bp *Eco*RI-*Bam*HI fragment of pDR540 containing the *tac* promoter was ligated into the *Eco*RI and *Bam*HI sites of pUC42S to generate pDR42S. The nucleotide sequence of the *ptr* gene was confirmed by ABI PRISM 310 genetic analyzer (Perkin-Elmer Japan, Tokyo). PCR was performed with the GeneAmp PCR system 2400 (Perkin-Elmer Japan) using KOD polymerase (Toyobo) according to the procedures recommended by the supplier.

**Overproduction and purification.** An overproducing strain was constructed by transforming *E. coli* JM109 with plasmid pDR42S. Cultivation was carried out at 37 °C until absorbance at 550 nm of the culture reached around 1.0. Induction of expression was done by adding 0.4 mM isopropyl- $\beta$ -D-thiogalactopyranoside (IPTG), and cultivation was continued for an additional 4-6 h. Cells were harvested by centrifugation and subjected to the following purification procedures.

Cells collected from 1-liter culture were suspended in 50 ml of 10 mM Tris-HCl (pH 8.0), disrupted by sonication using a model 450 Sonifier (Branson Ultrasonic, Danbury, CT, U.S.A.), and centrifuged at 15,000  $\times$  g for 30 min. The supernatant (crude extract) was dialyzed against 10 mM Tris-HCl (pH 8.0) and applied to a column (2.6  $\times$  15 cm) of DE-52 (Whatman Japan, Tokyo) equilibrated with the same buffer. After the column was washed, the enzyme was eluted with a linear gradient of 0 to 0.3 M NaCl. The enzyme fractions were pooled, concentrated by Centricon 10 centrifugal concentrators (Millipore Japan, Tokyo), and applied to a column (1.6  $\times$  190 cm) of Sephacryl S-300 (Amersham Biosciences) equilibrated with 10 mM Tris-HCl (pH 8.0) containing 0.1 M NaCl. The enzyme eluted from this column was used for biochemical characterizations. All purification procedures were carried out at 4 °C. The cellular production level and purity of the enzyme were analyzed by SDS-PAGE on 12% polyacrylamide gel,<sup>26)</sup> followed by staining with Coomassie Brilliant Blue.

**Enzymatic activity.** Stock solutions of various peptides (1.0 mg/ml) were prepared by dissolving the peptides contained in the vials (0.1-1 mg/vial) in 10 mM Tris-HCl (pH 8.0). An aliquot of each stock solution was used for the assay. The enzymatic reaction

was carried out in 500  $\mu\text{l}$  of 50 mM Tris-HCl (pH 8.0) containing 5–10  $\mu\text{g}$  of the peptide and an appropriate amount of the enzyme at 37 °C for 10 min, unless stated otherwise. The reaction was terminated by adding 10  $\mu\text{l}$  of glacial acetic acid. The reaction mixture was then subjected to reverse-phase HPLC to separate the products from the substrate. The amount of substrate digested by the enzyme was determined by comparing the peak areas of the substrate incubated with and without the enzyme. A response factor (peak area/ $\mu\text{g}$ ) was determined for each peptide by injecting several aliquots (1–10  $\mu\text{g}$ ) of the stock solutions onto the HPLC. All the peptides examined were stable upon incubation at 37 °C for 10 min. One unit of enzymatic activity was defined as the amount of the enzyme that degrades 1 nmol of the peptide per min at 37 °C. Specific activity was defined as enzymatic activity per mg of pitrilysin. For determination of kinetic parameters, enzymatic activity was determined at various substrate concentrations, which were varied in such a way that they spanned the  $K_m$  value (0.15, 0.29, 0.58, 1.2, 2.9, and 11.5  $\mu\text{M}$  for  $\beta$ -endorphin). The amount of the enzyme was controlled in such a way that the fraction of the substrate digested did not exceed 30% of the total. Under this condition, the amount of the substrate decreased in proportion to increases in the amount of the enzyme or the reaction time.

Protein concentration was determined by measuring UV absorption on the basis that the absorbance at 280 nm of a 0.1% solution is 1.18. This value was calculated by using  $\epsilon$  values of 1,576  $\text{M}^{-1}\text{cm}^{-1}$  for tyrosine and 5,225  $\text{M}^{-1}\text{cm}^{-1}$  for tryptophan at 280 nm.<sup>27)</sup>

**Reverse-phase HPLC.** Reverse-phase HPLC was carried out on a column (4.6  $\times$  250 mm) of Aquapore RP-300 (Brownlee Laboratories, Santa Clara, CA, U.S.A). Elution was performed by increasing linearly the concentration of solvent B in solvent A from 10% (v/v) to 60% (v/v) over 25 min, unless stated otherwise. Solvent A was 0.1% (v/v) trifluoroacetic acid and solvent B was acetonitrile containing 0.05% (v/v) trifluoroacetic acid. A flow rate of 1.0 ml/min was used and the peptides were detected with a UV detector set at 230 nm.

**Amino acid sequence and composition.** The  $\text{NH}_2$ -terminal amino acid sequence was determined using a Procise 491 automated protein sequencer (Perkin-Elmer Japan). Amino acid composition was determined using a Beckman System 6300E automatic amino acid analyzer (Tokyo, Japan). Samples were hydrolyzed at 150 °C for 1.5 h using a vapor-phase hydrolysis technique with constant-boiling HCl containing 0.5% (v/v) phenol.

**Circular dichroism spectra.** The circular dichroism (CD) spectra were measured using a J-725 spectropolarimeter (Japan Spectroscopic, Tokyo, Japan) at 25 °C

in 10 mM Tris-HCl (pH 8.0). For measurement of far- and near-UV CD spectra, a protein concentration of 0.1 mg/ml and 0.5–1 mg/ml with a cell optical path length of 2 mm and 10 mm were used, respectively. The mean residue ellipticity ( $\theta$ ,  $\text{deg cm}^2\text{dmol}^{-1}$ ) was calculated using an average amino acid molecular weight of 110.

## Results

### *Purification of the enzyme*

Upon induction for overproduction, pitrilysin accumulated in the cells in a soluble form. The overproducing strain grew almost similarly with the host strain, indicating that overproduction of this protein does not cause any significant damage to the cell. The production level was estimated to be approximately 70 mg/l culture by SDS-PAGE based on the intensity of the band visualized with Coomassie Brilliant Blue. The enzyme was purified by sonication lysis of the cells, followed by ion-exchange and gel filtration column chromatographies, to a monomeric form that gave a single band on SDS-PAGE (Fig. 1). The overall purification yield was 50%, with approximately 35 mg of the enzyme obtained from 1-liter culture. This amount is 70-fold<sup>8)</sup> and 2000-fold<sup>1)</sup> higher than those previously reported. The N-terminal amino acid sequence of the purified enzyme was found to be Glu-Thr-Gly-Trp-Gln-Pro-Ile-Gln-Glu, indicating that the purified enzyme represents a mature form of the enzyme in which the signal peptide (Met<sup>1</sup>-Ala<sup>23</sup>) was removed.

### *CD spectra*

The far- and near-UV CD spectra of the enzyme are shown in Fig. 2. The far-UV spectrum gave a broad trough with double minimum  $\theta$  values of  $-12,500$  at 209 nm and  $-12,800$  at 219 nm (Fig. 2A). The near-UV CD spectrum gave two positive peaks with maximum  $\theta$  values of 89 at 258 nm and 67 at 296 nm, and one

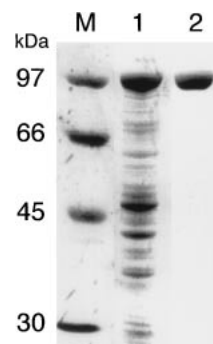


**Fig. 1.** SDS-PAGE of Pitrilysin Overproduced in *E. coli* Cells.

Samples were subjected to 12% SDS-PAGE and stained with Coomassie Brilliant Blue. Lane M, a low molecular weight marker kit (Amersham Biosciences); lane 1, whole cell extract; lane 2, purified pitrilysin. Numbers along the gel represent the molecular masses of the standard proteins.

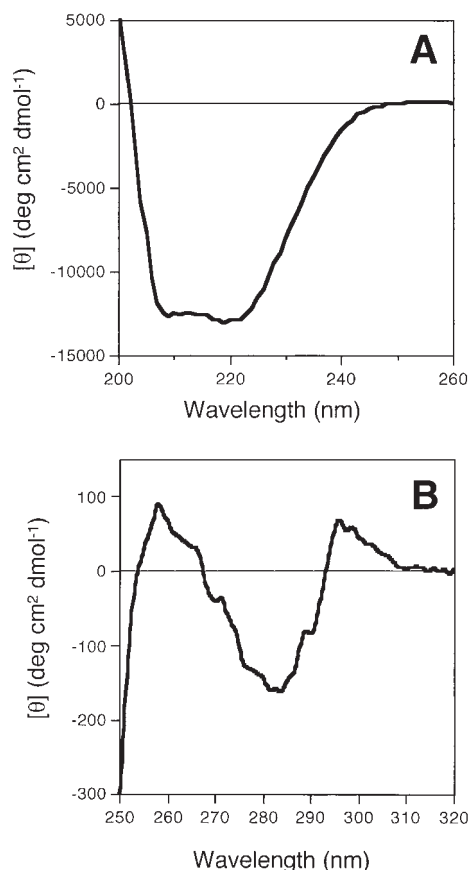


**Fig. 2.** CD Spectra of Pitrilysin.

The far-UV (A) and near-UV (B) CD spectra of pitrilysin are shown. These spectra were measured as described under "Experimental Procedures".

trough with a minimum  $\theta$  value of  $-160$  at  $282\text{ nm}$  (Fig. 2B). The helical content of the enzyme was calculated to be  $40.1\%$  using the method of Wu *et al.*<sup>28)</sup> It has been reported that a catalytically essential divalent cation binds to the enzyme too tightly to be removed by dialysis but can be removed upon EDTA treatment.<sup>2)</sup> To determine whether this divalent cation is important for the protein structure, the far- and near-UV CD spectra of the enzyme were measured in the presence of  $10\text{ mM}$  EDTA. However, both spectra were basically identical to those obtained in the absence of EDTA, indicating that the protein conformation was not markedly changed upon removal of the divalent cation from the active site.

#### *Enzymatic activities for various peptides*

Various peptides were cleaved by the enzyme at  $\text{pH } 8.0$  at  $37^\circ\text{C}$  without a divalent cation. This condition was used for the following reasons. (i) The enzyme was fully active over a broad  $\text{pH}$  range from  $7$  to  $9$  without a sharp  $\text{pH}$  optimum (data not shown). (ii) The enzyme has been reported to be unstable above  $50^\circ\text{C}$ .<sup>2)</sup> (iii) The enzymatic activities determined in the absence and presence of a catalytically essential divalent cation were nearly equal, probably because the purified enzyme

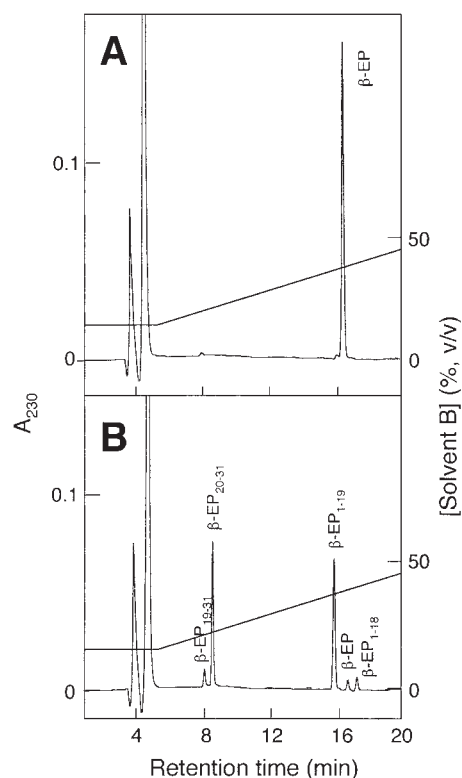


**Fig. 3.** Separation of Peptides by Reverse-phase HPLC.

$\beta\text{-EP}$  ( $10\ \mu\text{g}$ ,  $2.9\ \text{nmol}$ ) was incubated in the absence (A) or presence (B) of  $50\ \text{ng}$  of pitrilysin in  $500\ \mu\text{l}$  of  $50\ \text{mM}$  Tris-HCl ( $\text{pH } 8.0$ ) at  $37^\circ\text{C}$  for  $10\ \text{min}$ . After the enzymatic reaction was terminated by the addition of  $10\ \mu\text{l}$  of acetic acid, the reaction mixture was subjected to reverse-phase HPLC. The reverse-phase HPLC was carried out as described under "Experimental Procedures". The positions of  $\beta\text{-EP}$  and its degradation products are shown.

contains this divalent cation, which binds to the enzyme too tightly to be dissociated from the enzyme by dialysis. The amount of the substrate cleaved by the enzyme was determined by applying the reaction mixture to HPLC. As a typical example, separation of  $\beta\text{-EP}$  from its digestion products by HPLC is shown in Fig. 3. The enzyme cleaved all the peptides examined except for angiotensin I and bradykinin. It exhibited the highest specific activity, of  $6,200 \pm 500$  units/mg, for  $\beta\text{-EP}$ . The specific activities of the enzyme for other peptides relative to that for  $\beta\text{-EP}$  are summarized in Table 1. The specific activities of the enzyme for VIP, substance P, and glucagon relative to that for insulin B were  $42$ ,  $10$ , and  $8\%$ , respectively, comparable to those ( $23$ ,  $7$ , and  $11\%$ , respectively) reported previously.<sup>1)</sup> The enzyme cleaved  $\beta\text{-amyloid}$ , which plays a central role in the pathogenesis Alzheimer's disease, with relatively high efficiency.

To examine whether high activity of the enzyme toward  $\beta\text{-EP}$  results from high binding affinity, degradations of  $\beta\text{-EP}$ ,  $\beta\text{-amyloid}$ , insulin B, VIP, calcitonin, and substance P by the enzyme were analyzed kinetically. These peptides are cleaved by the enzyme predominantly at a single site, as shown below. The



**Table 1.** Enzymatic Activities of Pitrilysin for Cleavage of Various Peptides

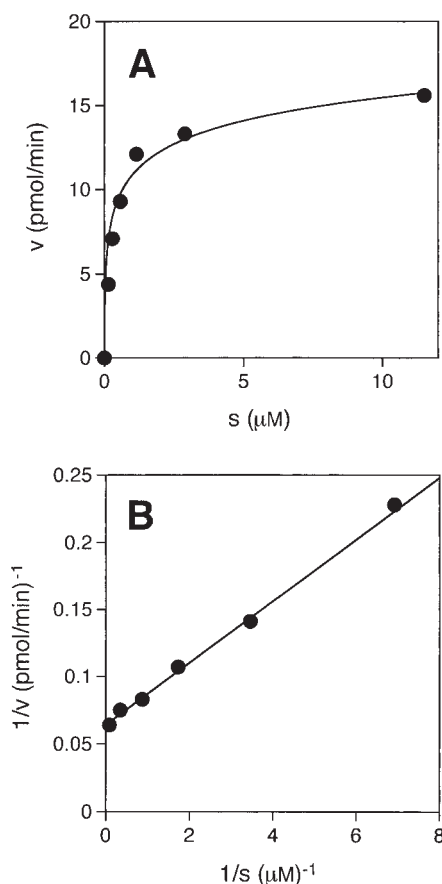
Peptide	Relative activity (%)	$K_m$ ( $\mu\text{M}$ )	$k_{\text{cat}}$ ( $\text{min}^{-1}$ )
$\beta$ -EP	100	$0.36 \pm 0.03$	$750 \pm 60$
$\beta$ -Amyloid	$18 \pm 3$	$0.90 \pm 0.1$	$140 \pm 15$
Insulin B	$17 \pm 3$	$1.5 \pm 0.1$	$160 \pm 15$
Insulin B <sub>1-22</sub>	$8.2 \pm 1$	$23 \pm 3$	$110 \pm 12$
Leumorphin	$15 \pm 2$	ND	ND
VIP	$7.2 \pm 1$	$0.40 \pm 0.04$	$54 \pm 6$
Calcitonin	$3.0 \pm 0.5$	$2.2 \pm 0.2$	$26 \pm 3$
Substance P	$1.7 \pm 0.3$	$31 \pm 3$	$38 \pm 4$
Glucagon	$1.4 \pm 0.2$	ND	ND
$\alpha$ ANP	$1.4 \pm 0.2$	ND	ND
ACTH	$1.0 \pm 0.2$	ND	ND
Somatostatin	$0.9 \pm 0.1$	ND	ND
Angiotensin I	<0.2		
Bradykinin	<0.2		

Enzymatic activity was determined at 37°C in 50 mM Tris-HCl (pH 8.0). The amount of the peptide cleaved by the enzyme was determined by HPLC, as described under "Experimental Procedures". Relative activity was calculated by dividing the specific activity of the enzyme for each peptide by that for  $\beta$ -EP ( $6,200 \pm 500$  units/mg). The kinetic parameters were determined by least-square fitting of the data obtained from Lineweaver-Burk plots. Results are shown with the standard deviations. ND, not determined.

rate of cleavage as a function of substrate concentration for  $\beta$ -EP is shown in Fig. 4A as a typical example. The kinetic parameters for  $\beta$ -EP were determined from the double reciprocal plot  $1/v$  versus  $1/s$  (Lineweaver-Burk plots) shown in Fig. 4B. Cleavage of other peptides by the enzyme also followed Michaelis-Menten kinetics, and the kinetic parameters were determined from corresponding Lineweaver-Burk plots (data not shown). These results are summarized in Table 1. The enzyme gave lowest  $K_m$  value of  $0.36 \pm 0.03 \mu\text{M}$  and a highest  $k_{\text{cat}}$  value of  $750 \pm 60 \text{ min}^{-1}$  for  $\beta$ -EP, indicating that  $\beta$ -EP is the most preferable substrate for pitrilysin. This  $K_m$  value increased by 2.5-fold for  $\beta$ -amyloid, 4.2-fold for insulin B, 1.1-fold for VIP, 6.1-fold for calcitonin, and 86-fold for substance P, indicating that the binding affinity of pitrilysin for substance P is greatly reduced as compared to that for  $\beta$ -EP. The kinetic parameters were also determined for insulin B<sub>1-22</sub>, which lacks the C-terminal eight residues of insulin B. This peptide was produced upon tryptic digestion of insulin B and purified by reverse-phase HPLC. The  $K_m$  value for insulin B<sub>1-22</sub> increased 15-fold as compared to that for insulin B, whereas the  $k_{\text{cat}}$  value for insulin B<sub>1-22</sub> was comparable to that for insulin B (Table 1). These results indicate that the C-terminal region of insulin B is important for the binding of pitrilysin.

#### Cleavage sites in the peptides

The cleavage sites in the substrates were determined by identifying the digestion products, which were separated by reverse-phase HPLC. Of the four digestion products of  $\beta$ -EP, for example, two major ones,  $\beta$ -EP<sub>1-19</sub> and  $\beta$ -EP<sub>20-31</sub>, and two minor ones,  $\beta$ -EP<sub>1-18</sub> and  $\beta$ -EP<sub>19-31</sub>, were identified (Fig. 3). This indicates that

**Fig. 4.** Rate of Cleavage as a Function of Substrate Concentration.

Various concentrations of  $\beta$ -EP were incubated with pitrilysin (4.4 ng) at 37°C for 10 min. The amount of the substrate degraded was determined by reverse-phase HPLC, as described under "Experimental Procedures". The experiments were carried out in duplicate, and the average values are indicated. The errors are within 15% of the values indicated. A plot of  $v$  versus  $s$  (A) and a double reciprocal plot of the data (B) are shown.

Lys<sup>19</sup>-Asn<sup>20</sup> and Phe<sup>18</sup>-Lys<sup>19</sup> are the major and minor cleavage sites, respectively, in  $\beta$ -EP. The amounts of the major digestion products were approximately 10 times higher than those of the minor ones. The time dependence of the cleavage reaction shows that this ratio is unchanged regardless of whether  $\beta$ -EP is partially or almost fully cleaved (data not shown). These results indicate that pitrilysin predominantly cleaves  $\beta$ -EP at the Lys<sup>19</sup>-Asn<sup>20</sup> site. The major cleavage sites in the peptides thus determined are shown in Fig. 5. These include Lys<sup>19</sup>-Asn<sup>20</sup> for  $\beta$ -EP, His<sup>14</sup>-Gln<sup>15</sup> for  $\beta$ -amyloid, Tyr<sup>16</sup>-Leu<sup>17</sup> for insulin B, Arg<sup>6</sup>-Arg<sup>7</sup> and Thr<sup>13</sup>-Arg<sup>14</sup> for leumorphin, Arg<sup>14</sup>-Lys<sup>15</sup> for VIP, His<sup>20</sup>-Thr<sup>21</sup> for calcitonin, Gly<sup>9</sup>-Leu<sup>10</sup> for substance P, Phe<sup>6</sup>-Thr<sup>7</sup> and Lys<sup>12</sup>-Tyr<sup>13</sup> for glucagon, Leu<sup>2</sup>-Arg<sup>3</sup>, Arg<sup>14</sup>-Ile<sup>15</sup>, and Gly<sup>22</sup>-Cys<sup>23</sup> for  $\alpha$ ANP, Tyr<sup>2</sup>-Ser<sup>3</sup> for ACTH, and Phe<sup>17</sup>-Phe<sup>18</sup> and Trp<sup>19</sup>-Lys<sup>20</sup> for somatostatin.  $\beta$ -Amyloid, insulin B, leumorphin, VIP, and somatostatin were almost exclusively cleaved at the above mentioned sites, whereas other peptides were cleaved with less efficiency at additional sites, such as

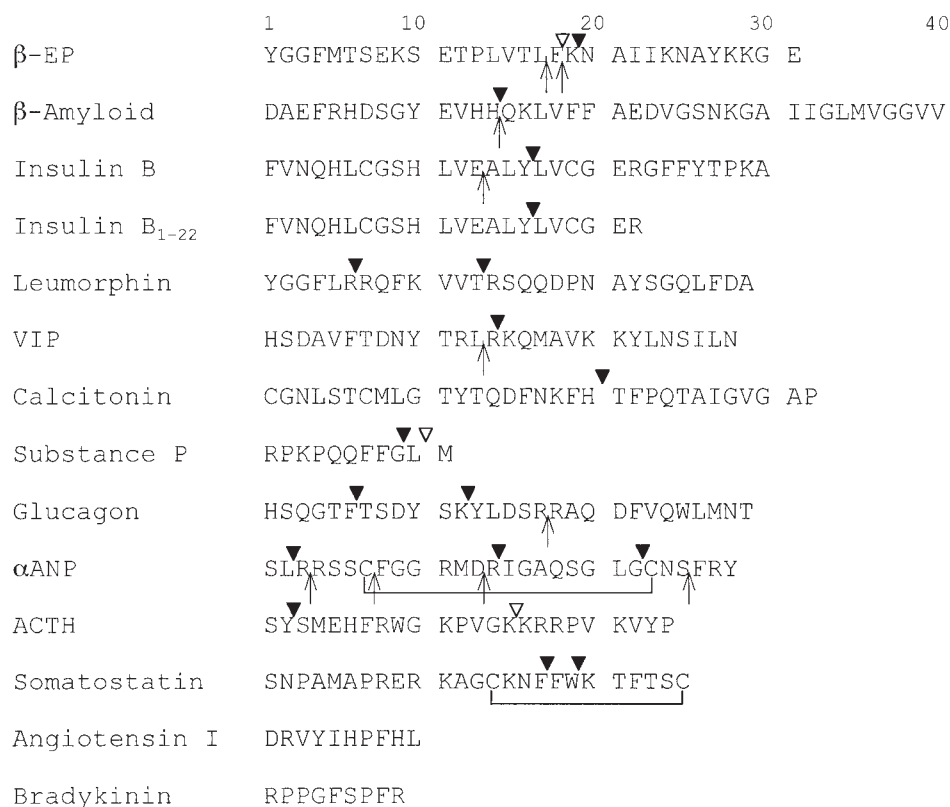


**Fig. 5.** The Cleavage Sites in the Peptides.

The major (solid triangle) and minor (open triangle) cleavage sites by pitrilysin are indicated above the sequences of the peptides. Angiotensin I and bradykinin were not cleaved by the enzyme. The cleavage sites by insulysin in  $\beta$ -EP,<sup>36)</sup> insulin B,<sup>36)</sup>  $\beta$ -amyloid,<sup>39)</sup> glucagon,<sup>32)</sup> and  $\alpha$ ANP<sup>34)</sup> are indicated by arrows below the sequences. The positions of disulfide bonds are also shown.

Phe<sup>18</sup>-Lys<sup>19</sup> for  $\beta$ -EP, Phe<sup>8</sup>-Gly<sup>9</sup> for substance P, and Lys<sup>15</sup>-Lys<sup>16</sup> for ACTH. However, those for calcitonin, glucagon, and  $\alpha$ ANP remained to be identified. Insulin B was cleaved at the second site (Phe<sup>25</sup>-Tyr<sup>26</sup>), as reported previously,<sup>2)</sup> but this site was not cleaved at a detectable rate until the initial site (Tyr<sup>16</sup>-Leu<sup>17</sup>) was almost completely cleaved. The cleavage site in VIP is different from that (Leu<sup>13</sup>-Arg<sup>14</sup>) previously reported. The reason for this inconsistency remains to be answered.

Two amino acid residues flanking the cleavage site varied greatly among the various substrates, suggesting that pitrilysin does not have any side chain specificity for these residues (Fig. 5). To confirm this, the  $\beta$ -EP derivatives, [N<sup>19</sup>]- $\beta$ -EP and [A<sup>19</sup>]- $\beta$ -EP, in which Lys<sup>19</sup> is replaced by Asn and Ala, respectively, were analyzed for cleavage by the enzyme. The elution patterns of the resultant products from reverse-phase HPLC were similar to that for  $\beta$ -EP (data not shown), indicating that these peptides were predominantly cleaved at the Asn<sup>19</sup>-Asn<sup>20</sup> or the Ala<sup>19</sup>-Asn<sup>20</sup> site, but less at the Phe<sup>18</sup>-Lys<sup>19</sup> site. The specific activities of the enzyme for these  $\beta$ -EP derivatives were 80% of that for  $\beta$ -EP. Hence, alteration of the amino acid residue flanking the amino side of the cleavage site seriously affects neither the cleavage site in the substrate nor the susceptibility of  $\beta$ -EP to degradation by the enzyme.

#### Identification of the residues in $\beta$ -EP important for its binding to *E. coli* pitrilysin

To identify the residues in  $\beta$ -EP important for its binding to pitrilysin, a series of  $\beta$ -EP derivatives with N or C-terminal truncations were prepared and cleaved by the enzyme. The sequences of these peptides, as well as those of the  $\beta$ -EP derivatives with amino acid substitutions, are summarized in Table 2.  $\beta$ -EP<sub>9-31</sub>,  $\beta$ -EP<sub>14-31</sub>, and  $\beta$ -EP<sub>18-31</sub> lack the N-terminal 8, 13, and 17 amino acid residues of  $\beta$ -EP, respectively, while  $\beta$ -EP<sub>9-26</sub> and  $\beta$ -EP<sub>9-21</sub> lack the C-terminal 5 and 10 residues of  $\beta$ -EP<sub>9-31</sub>, respectively. The cleavage sites in these peptides were determined to be those in  $\beta$ -EP.  $\beta$ -EP<sub>9-31</sub> and  $\beta$ -EP<sub>14-31</sub> were cleaved at same two sites as in  $\beta$ -EP, whereas other peptides were cleaved almost exclusively at a single site (Lys<sup>19</sup>-Asn<sup>20</sup>). The kinetic parameters of the enzyme for a series of  $\beta$ -EP derivatives with N or C-terminal truncations are summarized in Table 3.

The  $k_{cat}$  values for the truncated forms of  $\beta$ -EP were comparable to that for  $\beta$ -EP, indicating that pitrilysin cleaves these peptides with similar hydrolysis rates. In contrast, the  $K_m$  values for these peptides increased as the size of the truncated region increased, suggesting that the entire region of  $\beta$ -EP is involved in binding to the enzyme, but the  $K_m$  values for these peptides did not increase in proportion with the size of the truncated region. Truncation of eight N-terminal residues, for

**Table 2.** Sequences of the  $\beta$ -EP Derivatives

Peptide	Sequence			
	1	10	20	30
$\beta$ -EP	YGGFMTSEKS	ETPLVTLFKN	AIKKNAYKKG	E
[N <sup>19</sup> ]- $\beta$ -EP	YGGFMTSEKS	ETPLVTLFNN	AIKKNAYKKG	E
[A <sup>19</sup> ]- $\beta$ -EP	YGGFMTSEKS	ETPLVTLFAN	AIKKNAYKKG	E
$\beta$ -EP <sub>9-31</sub>		KS	ETPLVTLFKN	AIKKNAYKKG E
$\beta$ -EP <sub>14-31</sub>			LVTLFKN	AIKKNAYKKG E
$\beta$ -EP <sub>18-31</sub>			FKN	AIKKNAYKKG E
$\beta$ -EP <sub>9-26</sub>		KS	ETPLVTLFKN	AIKNA
$\beta$ -EP <sub>9-21</sub>		KS	ETPLVTLFKN	A
[S <sup>14</sup> /S <sup>15</sup> /S <sup>17</sup> ]- $\beta$ -EP <sub>9-26</sub>		KS	ETPSSTSFKN	AIKNA
[S <sup>14</sup> ]- $\beta$ -EP <sub>9-26</sub>		KS	ETPSVTTLFKN	AIKNA
[S <sup>15</sup> ]- $\beta$ -EP <sub>9-26</sub>		KS	ETPLSTLTKN	AIKNA
[S <sup>17</sup> ]- $\beta$ -EP <sub>9-26</sub>		KS	ETPLVTSFKN	AIKNA
[S <sup>22</sup> /S <sup>23</sup> ]- $\beta$ -EP <sub>9-26</sub>		KS	ETPLVTLFKN	ASSKNA

The asparagine and alanine residues substituted for Lys<sup>19</sup> and the serine residues substituted for hydrophobic residues at positions 14, 15, 17, 22, and 23 are underlined.

**Table 3.** Kinetic Parameters of Pitrilysin for Cleavage of  $\beta$ -Endorphin Derivatives

Peptide	$K_m$ ( $\mu$ M)	$k_{cat}$ (min <sup>-1</sup> )	Relative $k_{cat}$ (%)
$\beta$ -EP	0.36 $\pm$ 0.03	750 $\pm$ 60	100
$\beta$ -EP <sub>9-31</sub>	0.85 $\pm$ 0.08	640 $\pm$ 60	85
$\beta$ -EP <sub>14-31</sub>	3.3 $\pm$ 0.4	820 $\pm$ 90	109
$\beta$ -EP <sub>18-31</sub>	65 $\pm$ 8	680 $\pm$ 80	91
$\beta$ -EP <sub>9-26</sub>	2.7 $\pm$ 0.3	670 $\pm$ 70	89 (100)
$\beta$ -EP <sub>9-21</sub>	98 $\pm$ 10	810 $\pm$ 90	108
[S <sup>14</sup> /S <sup>15</sup> /S <sup>17</sup> ]- $\beta$ -EP <sub>9-26</sub>	200 $\pm$ 20	5.3 $\pm$ 0.5	0.7 (0.8)
[S <sup>14</sup> ]- $\beta$ -EP <sub>9-26</sub>	11 $\pm$ 1	44 $\pm$ 5	5.9 (6.6)
[S <sup>15</sup> ]- $\beta$ -EP <sub>9-26</sub>	9.3 $\pm$ 1	97 $\pm$ 10	13 (14)
[S <sup>17</sup> ]- $\beta$ -EP <sub>9-26</sub>	14 $\pm$ 2	49 $\pm$ 5	6.5 (7.3)
[S <sup>22</sup> /S <sup>23</sup> ]- $\beta$ -EP <sub>9-26</sub>	1.4 $\pm$ 0.2	340 $\pm$ 40	45 (51)

Enzymatic activity was determined at 37 °C in 50 mM Tris-HCl (pH 8.0). The kinetic parameters were determined by least-square fitting of the data obtained from Lineweaver-Burk plots. Relative  $k_{cat}$  values were calculated by dividing the  $k_{cat}$  value for each peptide by that for  $\beta$ -EP. The  $k_{cat}$  value for each peptide relative to that for  $\beta$ -EP<sub>9-26</sub> is shown in parentheses. Results are shown with the standard deviations.

example, increased the  $K_m$  value by 2.4-fold. Subsequent truncation of five additional residues increased it by 3.9-fold, while further truncation of four more residues increased it greatly, by 20-fold. Likewise, truncation of five C-terminal residues increased the  $K_m$  value by 3.2-fold, while further truncation of five additional residues greatly increased it, by 36-fold. These results indicate that regions 14–17 and 22–26 in  $\beta$ -EP are responsible for high-affinity recognition by pitrilysin.

Region 14–17 contains three hydrophobic residues. To examine the importance of these residues for the binding of  $\beta$ -EP to pitrilysin, a series of  $\beta$ -EP<sub>9-26</sub> derivatives, in which Leu<sup>14</sup>, Val<sup>15</sup>, and Leu<sup>17</sup> are individually or simultaneously replaced by Ser, were cleaved by the enzyme. [S<sup>14</sup>], [S<sup>15</sup>], and [S<sup>17</sup>]- $\beta$ -EP<sub>9-26</sub> represent the  $\beta$ -EP<sub>9-26</sub> derivatives with single replacement at positions 14, 15, and 17, respectively. [S<sup>14</sup>/S<sup>15</sup>/S<sup>17</sup>]- $\beta$ -EP<sub>9-26</sub> represents the one with triple replace-

ments (Table 2). The kinetic parameters of the enzyme for these peptides are summarized in Table 3. Single replacement results in a 3.4 to 5.2-fold increase in the  $K_m$  value, along with a 7 to 15-fold decrease in the  $k_{cat}$  value. The effects of single replacements were cumulative, and replacement of all three residues resulted in a 74-fold increase in the  $K_m$  value along with a 130-fold decrease in the  $k_{cat}$  value. These results suggest that the hydrophobic residues located at positions 14, 15, and 17 of  $\beta$ -EP are important for binding to pitrilysin. The hydrophobic residues are also present in region 22–26 (Ile<sup>22</sup> and Ile<sup>23</sup>), but the  $k_{cat}/K_m$  value of the enzyme for [S<sup>22</sup>/S<sup>23</sup>]- $\beta$ -EP<sub>9-26</sub>, in which these residues are simultaneously replaced by Ser, was similar to that for  $\beta$ -EP<sub>9-26</sub> (Table 3). These results suggest that Ile<sup>22</sup> and Ile<sup>23</sup> are not important for the binding of  $\beta$ -EP to pitrilysin.

## Discussion

### Comparison of substrate and cleavage-site specificities of pitrilysin with those of insulysin

Insulysin (insulin-degrading enzyme, IDE), which is a dimeric or trimeric enzyme,<sup>29</sup> has been reported to degrade not only insulin<sup>30</sup> but also other peptide hormones, such as glucagon,<sup>31,32</sup>  $\alpha$ ANP,<sup>33,34</sup> transforming growth factor  $\alpha$  (TGF- $\alpha$ ),<sup>35</sup>  $\beta$ -EP,<sup>36</sup> and calcitonin.<sup>31</sup> It also cleaves  $\beta$ -amyloid peptides.<sup>37–39</sup> Insulysin cleaves these peptides at a limited number of sites. However, because no apparent amino acid sequence identities were observed around the cleavage sites, it has been proposed that insulysin recognizes secondary or tertiary structures of these peptides.<sup>29,40</sup> The peptides examined for degradation by pitrilysin include these insulysin substrates, except for TGF- $\alpha$ , as well as non-insulysin substrates,<sup>36</sup> such as ACTH, angiotensin I, and bradykinin. Pitrilysin degraded these insulysin substrates but did not degrade or poorly degraded non-insulysin substrates. Furthermore, pitrilysin degraded these peptides at a limited number of sites, as did insulysin. These results strongly suggest that pitrilysin and insulysin

recognize these substrates by a similar mechanism. However, these two enzymes differ in substrate and cleavage-site specificities.

Of the peptides, for which the kinetic parameters of pitrilysin were determined,  $\beta$ -EP and insulin B are the only ones for which the kinetic parameters of insulysin are available. The  $K_m$  and  $k_{cat}$  values of insulysin have been reported to be  $13 \mu\text{M}$  and  $21 \text{min}^{-1}$  for  $\beta$ -EP ( $k_{cat}/K_m$  of  $1.6 \text{min}^{-1}/\mu\text{M}$ ), and  $0.47 \mu\text{M}$  and  $7.8 \text{min}^{-1}$  for insulin B ( $k_{cat}/K_m$  of  $17 \text{min}^{-1}/\mu\text{M}$ ).<sup>36</sup> The  $K_m$  and  $k_{cat}$  values of pitrilysin were determined to be  $0.36 \mu\text{M}$  and  $750 \text{min}^{-1}$  for  $\beta$ -EP ( $k_{cat}/K_m$  of  $2100 \text{min}^{-1}/\mu\text{M}$ ), and  $1.5 \mu\text{M}$  and  $160 \text{min}^{-1}$  for insulin B ( $k_{cat}/K_m$  of  $110 \text{min}^{-1}/\mu\text{M}$ ). Thus, on the basis of  $k_{cat}/K_m$  values, pitrilysin prefers  $\beta$ -EP to insulin B whereas insulysin prefers insulin B to  $\beta$ -EP. This difference might arise from a difference in the binding affinities of the peptides, because  $\beta$ -EP exhibits a 4.2-fold increased affinity for pitrilysin and a 28-fold decreased affinity for insulysin relative to insulin B. Both enzymes degrade  $\beta$ -EP at a hydrolysis rate higher than that for insulin B. Similar results have been reported previously, in which insulysin degrades insulin more efficiently than IGF II whereas pitrilysin degrades them equally.<sup>4</sup> Cross-linking studies suggest that insulin and IGF II differ in their binding affinity for insulysin (insulin > IGF II), while they exhibit similar binding affinities for pitrilysin. The  $K_m$  value of pitrilysin for insulin B determined in our study was smaller than but comparable to that ( $7.1 \mu\text{M}$ ) reported previously.<sup>36</sup>

The major cleavage sites of insulysin in the following peptides have been reported as Glu<sup>13</sup>-Ala<sup>14</sup> for insulin B,<sup>36</sup> His<sup>14</sup>-Gln<sup>15</sup> for  $\beta$ -amyloid,<sup>39</sup> Leu<sup>17</sup>-Phe<sup>18</sup> and Phe<sup>18</sup>-Lys<sup>19</sup> for  $\beta$ -EP,<sup>36</sup> Arg<sup>17</sup>-Arg<sup>18</sup> for glucagon,<sup>32</sup> and Arg<sup>3</sup>-Arg<sup>4</sup>, Cys<sup>7</sup>-Phe<sup>8</sup>, Asp<sup>13</sup>-Arg<sup>14</sup>, and Ser<sup>25</sup>-Phe<sup>26</sup> for  $\alpha$ ANP.<sup>34</sup> Of these sites, only His<sup>14</sup>-Gln<sup>15</sup> for  $\beta$ -amyloid is shared with pitrilysin, although several sites located close to the major cleavage sites of insulysin were also cleaved by pitrilysin (Fig. 5). The difference in the subunit structures and/or the structures of the substrate-binding sites of pitrilysin and insulysin might be responsible for the differences in substrate and cleavage-site specificities of these enzymes.

The  $K_m$  and  $k_{cat}$  values for cleavage of insulin have been reported to be  $1.1 \mu\text{M}$  and  $1.8 \text{min}^{-1}$  ( $k_{cat}/K_m$  of  $1.6 \text{min}^{-1}/\mu\text{M}$ ) for pitrilysin,<sup>1</sup> and  $0.13 \mu\text{M}$  and  $0.56 \text{min}^{-1}$  ( $k_{cat}/K_m$  of  $4.3 \text{min}^{-1}/\mu\text{M}$ ) for insulysin.<sup>36</sup> These results suggest that pitrilysin and insulysin cleave insulin with similar efficiency. The major cleavage sites in insulin by insulysin have been reported to be Leu<sup>13</sup>-Tyr<sup>14</sup> and Tyr<sup>14</sup>-Gln<sup>15</sup> in the A chain, and Ser<sup>9</sup>-His<sup>10</sup>, Glu<sup>13</sup>-Ala<sup>14</sup>, Tyr<sup>16</sup>-Leu<sup>17</sup>, and Phe<sup>25</sup>-Tyr<sup>26</sup> in the B chain.<sup>30</sup> Of these, Tyr<sup>14</sup>-Gln<sup>15</sup> in the A chain and Tyr<sup>16</sup>-Leu<sup>17</sup> in the B chain are shared with pitrilysin (A. Kohara, unpublished result).

#### *Substrate recognition mechanism*

Kinetic analyses of pitrilysin using a series of  $\beta$ -EP

derivatives with N- and/or C-terminal truncations indicated that regions 14–17 and 22–26 in  $\beta$ -EP are responsible for high affinity recognition by pitrilysin. Three hydrophobic residues located at region 14–17 (Leu<sup>14</sup>, Val<sup>15</sup>, and Leu<sup>17</sup>) in  $\beta$ -EP were found to be important for binding of  $\beta$ -EP to pitrilysin. The degree of decrease in affinity by substitution of all these residues with a hydrophilic one (Ser) was comparable to that by truncation of region 14–17. In contrast, two hydrophobic residues located at region 22–26 (Ile<sup>22</sup> and Ile<sup>23</sup>) were shown not to be important for the binding of  $\beta$ -EP to pitrilysin. These results suggest that hydrophobic interactions are important for the binding of  $\beta$ -EP to pitrilysin at region 14–17, whereas other interactions are important for the binding of  $\beta$ -EP to pitrilysin at region 22–26.

Because regions 14–17 and 22–26 are located on the N- and C-terminal sides of the cleavage site in  $\beta$ -EP, the substrate binding site of pitrilysin probably consists of at least two sites, S and S'. The S and S' sites are responsible for binding to the P and P' residues of the substrates, which are located at the N- and C-terminal regions of the cleavage site, respectively. This structural feature of the binding site of pitrilysin might account for the large  $K_m$  value for substance P. This is because substance P is cleaved by pitrilysin at its C-terminal region and therefore does not have the C-terminal extension required for binding to the S' site of pitrilysin. In fact, the  $K_m$  value of pitrilysin for substance P ( $31 \mu\text{M}$ ) was comparable to those for  $\beta$ -EP<sub>18–31</sub> ( $65 \mu\text{M}$ ) and  $\beta$ -EP<sub>9–21</sub> ( $98 \mu\text{M}$ ), which do not have the N-terminal and C-terminal extensions required for binding to the S and S' sites of pitrilysin, respectively.

No similarity is observed in the amino acid sequences around the cleavage sites of the peptides by pitrilysin (Fig. 5). For example, Leu<sup>14</sup>, Val<sup>15</sup>, and Leu<sup>17</sup> of  $\beta$ -EP are located at the 6th, 5th, and 3rd positions from the cleavage site (N-terminal side). When the amino acid residues located at the corresponding positions of other substrates are compared, they vary greatly in size and hydrophobicity. These results strongly suggest that pitrilysin does not recognize the primary structure of the substrate, but recognizes its secondary or tertiary structures, as suggested for insulysin. However, the far-UV CD spectra of  $\beta$ -EP and insulin B measured under a condition under which these peptides are cleaved by pitrilysin indicated that both peptides assume a random coil-like structure (data not shown). These spectra were not significantly changed either in the presence of  $1 \text{mM}$  ZnCl<sub>2</sub> or  $10 \text{mM}$  EDTA, indicating that the conformation of the peptide is not seriously changed in the presence of the metal cofactor for pitrilysin activity. Thus, the question arises whether the secondary or the tertiary structure of the peptide is induced upon binding to pitrilysin. To answer this question, X-ray crystallographic studies of pitrilysin both in substrate-free and substrate-bound forms are necessary. Ease of overproduction and purification of the enzyme in amounts



sufficient for structural studies would facilitate these studies. Understanding of the mechanism by which pitrilysin recognizes the substrates would offer insight into the substrate-recognition mechanism of insulysin.

The C-terminal region of insulin B (residues 23–30) was found to be important for binding to pitrilysin. This region includes the Phe–Phe–Tyr sequence at 24–26, which has been shown to be important for the binding of insulin to insulysin.<sup>41)</sup> However, it remains to be determined whether this sequence is also important for the binding of insulin B to pitrilysin, because insulin B is almost exclusively cleaved by pitrilysin at the Tyr<sup>16</sup>–Leu<sup>17</sup> site, while insulin is cleaved by insulysin at additional sites, including Phe<sup>25</sup>–Tyr<sup>26</sup>. Further studies are necessary to identify the residues important for the binding of insulin B to pitrilysin.

#### Possible physiological role

It is obvious that the peptides examined for degradation by pitrilysin in this study are not the natural substrates for this enzyme, but the observation that pitrilysin degrades these peptides with a similar mechanism to that of insulysin allows us to propose that characteristics common to the insulysin substrates are shared by the pitrilysin substrates. It has been suggested that insulysin functions as a scavenger of protein fragments prone to form aggregates and amyloids.<sup>25,42)</sup> Hence, it is plausible to speculate that peptides with high aggregation potential can be natural substrates for pitrilysin. These peptides should be rapidly degraded, because accumulation of them in the periplasm, followed by the formation of aggregates might prevent normal cell growth. Signal peptides, which are processed from precursor proteins upon secretion, are one of the candidates for natural pitrilysin substrates, because pitrilysin family metallopeptidases have been shown to be involved in the degradation of a signal peptide released from a precursor protein in peroxisome,<sup>42)</sup> chloroplast,<sup>15)</sup> and mitochondria.<sup>13)</sup> Misfolded proteins are another candidate, because pitrilysin has been shown to be involved in the degradation of misfolded maltose-binding protein in the periplasm.<sup>43)</sup>

#### Acknowledgments

This work was supported in part by Grants-in-Aid for National Project on Protein Structure and Functional Analyses (to S.K.), for Scientific Research (no. 16041229) (to S.K.), and for Scientific Research in Priority Areas (C) “Genome Information Science” (to K.T.) from the Ministry of Education, Culture, Sports, Science, and Technology of Japan.

#### References

- 1) Anastasi, A., Knight, C. G., and Barrett, A. J., Characterization of the bacterial metalloendopeptidase pitrilysin by use of a continuous fluorescence assay. *Biochem. J.*, **290**, 601–607 (1993).

- 2) Cheng, Y. S., and Zipser, D., Purification and characterization of protease III from *Escherichia coli*. *J. Biol. Chem.*, **254**, 4698–4706 (1979).
- 3) Swamy, K. H., and Goldberg, A. L., Subcellular distribution of various proteases in *Escherichia coli*. *J. Bacteriol.*, **149**, 1027–1033 (1982).
- 4) Ding, L., Becker, A. B., Suzuki, A., and Roth, R. A., Comparison of the enzymatic and biochemical properties of human insulin-degrading enzyme and *Escherichia coli* protease III. *J. Biol. Chem.*, **267**, 2414–2420 (1992).
- 5) Dykstra, C. C., Prasher, D., and Kushner, S. R., Physical and biochemical analysis of the cloned *recB* and *recC* genes of *Escherichia coli* K-12. *J. Bacteriol.*, **157**, 21–27 (1984).
- 6) Cheng, Y. S., Zipser, D., Cheng, C. Y., and Rolseth, S. J., Isolation and characterization of mutations in the structural gene for protease III (*ptr*). *J. Bacteriol.*, **140**, 125–130 (1979).
- 7) Dykstra, C. C., and Kushner, S. R., Physical characterization of the cloned protease III gene from *Escherichia coli* K-12. *J. Bacteriol.*, **163**, 1055–1059 (1985).
- 8) Finch, P. W., Wilson, R. E., Brown, K., Hickson, I. D., and Emmerson, P. T., Complete nucleotide sequence of the *Escherichia coli ptr* gene encoding protease III. *Nucleic Acids Res.*, **14**, 7695–7703 (1986).
- 9) Affholter, J. A., Fried, V. A., and Roth, R. A., Human insulin-degrading enzyme shares structural and functional homologies with *E. coli* protease III. *Science*, **242**, 1415–1418 (1988).
- 10) Baumeister, H., Muller, D., Rehbein, M., and Richter, D., The rat insulin-degrading enzyme. Molecular cloning and characterization of tissue-specific transcripts. *FEBS Lett.*, **317**, 250–254 (1993).
- 11) Kuo, W. L., Gehm, B. D., and Rosner, M. R., Cloning and expression of the cDNA for a *Drosophila* insulin-degrading enzyme. *Mol. Endocrinol.*, **4**, 1580–1591 (1990).
- 12) Pierotti, A. R., Prat, A., Chesneau, V., Gaudoux, F., Leseney, A. M., Foulon, T., and Cohen, P., N-arginine dibasic convertase, a metalloendopeptidase as a prototype of a class of processing enzymes. *Proc. Natl. Acad. Sci. U.S.A.*, **91**, 6078–6082 (1994).
- 13) Stahl, A., Moberg, P., Ytterberg, J., Panfilov, O., Brockenhuus von Lowenhielm, H., Nilsson, F., and Glaser, E., Isolation and identification of a novel mitochondrial metalloprotease (PreP) that degrades targeting presequences in plants. *J. Biol. Chem.*, **277**, 41931–41939 (2002).
- 14) Mzhavia, N., Berman, Y. L., Qian, Y., Yan, L., and Devi, L. A., Cloning, expression, and characterization of human metalloprotease 1: a novel member of the pitrilysin family of metalloendopeptidases. *DNA Cell Biol.*, **18**, 369–380 (1999).
- 15) VanderVere, P. S., Bennett, T. M., Oblong, J. E., and Lamppa, G. K., A chloroplast processing enzyme involved in precursor maturation shares a zinc-binding motif with a recently recognized family of metalloendopeptidases. *Proc. Natl. Acad. Sci. U.S.A.*, **92**, 7177–7181 (1995).
- 16) Eggleston, K. K., Duffin, K. L., and Goldberg, D. E., Identification and characterization of calcylisin, a metallopeptidase involved in hemoglobin catabolism within

- the malaria parasite *Plasmodium falciparum*. *J. Biol. Chem.*, **274**, 32411–32417 (1999).
- 17) Fujita, A., Oka, C., Arikawa, Y., Katagai, T., Tonouchi, A., Kuhara, S., and Misumi, Y., A yeast gene necessary for bud-site selection encodes a protein similar to insulin-degrading enzymes. *Nature*, **372**, 567–570 (1994).
  - 18) Rawlings, N. D., Metalloprotease family. In “Handbook of Proteolytic Enzymes”, eds. Barret, A. J., Rawlings, N. D., and Woessner, J., Academic Press, Bath, U.K., pp. 1360–1362 (1998).
  - 19) Becker, A. B., and Roth, R. A., Insulysin and pitrilysin: insulin-degrading enzymes of mammals and bacteria. *Methods Enzymol.*, **248**, 693–703 (1995).
  - 20) Becker, A. B., and Roth, R. A., An unusual active site identified in a family of zinc metalloendopeptidases. *Proc. Natl. Acad. Sci. U.S.A.*, **89**, 3835–3839 (1992).
  - 21) Becker, A. B., and Roth, R. A., Identification of glutamate-169 as the third zinc-binding residue in proteinase III, a member of the family of insulin-degrading enzymes. *Biochem. J.*, **292**, 137–142 (1993).
  - 22) Perlman, R. K., Gehm, B. D., Kuo, W. L., and Rosner, M. R., Functional analysis of conserved residues in the active site of insulin-degrading enzyme. *J. Biol. Chem.*, **268**, 21538–21544 (1993).
  - 23) Perlman, R. K., and Rosner, M. R., Identification of zinc ligands of the insulin-degrading enzyme. *J. Biol. Chem.*, **269**, 33140–33145 (1994).
  - 24) Gehm, B. D., Kuo, W. L., Perlman, R. K., and Rosner, M. R., Mutations in a zinc-binding domain of human insulin-degrading enzyme eliminate catalytic activity but not insulin binding. *J. Biol. Chem.*, **268**, 7943–7948 (1993).
  - 25) Kurochkin, I. V., Insulin-degrading enzyme: embarking on amyloid destruction. *Trends Biochem. Sci.*, **26**, 421–425 (2001).
  - 26) Laemmli, U. K., Cleavage of structural proteins during the assembly of the head of bacteriophage T4. *Nature*, **227**, 680–685 (1970).
  - 27) Goodwin, T. W., and Morton, R. A., The spectrophotometric determination of tyrosine and tryptophan in proteins. *Biochem. J.*, **40**, 628–632 (1946).
  - 28) Wu, C.-S. C., Ikeda, K., and Yang, J. T., Ordered conformation of polypeptides and proteins in acidic dodecyl sulfate solution. *Biochemistry*, **20**, 566–570 (1981).
  - 29) Authier, F., Posner, B. I., and Bergeron, J. J., Insulin-degrading enzyme. *Clin. Invest. Med.*, **19**, 149–160 (1996).
  - 30) Duckworth, W. C., Hamel, F. G., Peavy, D. E., Liepnieks, J. J., Ryan, M. P., Hermodson, M. A., and Frank, B. H., Degradation products of insulin generated by hepatocytes and by insulin protease. *J. Biol. Chem.*, **263**, 1826–1833 (1988).
  - 31) Kirschner, R. J., and Goldberg, A. L., A high molecular weight metalloendoprotease from the cytosol of mammalian cells. *J. Biol. Chem.*, **258**, 967–976 (1983).
  - 32) Rose, K., Savoy, L. A., Muir, A. V., Davies, J. G., Offord, R. E., and Turcatti, G., Insulin proteinase liberates from glucagon a fragment known to have enhanced activity against  $\text{Ca}^{2+} + \text{Mg}^{2+}$ -dependent ATPase. *Biochem. J.*, **256**, 847–851 (1988).
  - 33) Muller, D., Baumeister, H., Buck, F., and Richter, D., Atrial natriuretic peptide (ANP) is a high-affinity substrate for rat insulin-degrading enzyme. *Eur. J. Biochem.*, **202**, 285–292 (1991).
  - 34) Muller, D., Schulze, C., Baumeister, H., Buck, F., and Richter, D., Rat insulin-degrading enzyme: cleavage pattern of the natriuretic peptide hormones ANP, BNP, and CNP revealed by HPLC and mass spectrometry. *Biochemistry*, **31**, 11138–11143 (1992).
  - 35) Hamel, F. G., Gehm, B. D., Rosner, M. R., and Duckworth, W. C., Identification of the cleavage sites of transforming growth factor  $\alpha$  by insulin-degrading enzymes. *Biochim. Biophys. Acta*, **1338**, 207–214 (1997).
  - 36) Safavi, A., Miller, B. C., Cottam, L., and Hersh, L. B., Identification of  $\gamma$ -endorphin-generating enzyme as insulin-degrading enzyme. *Biochemistry*, **35**, 14318–14325 (1996).
  - 37) Kurochkin, I. V., and Goto, S., Alzheimer's  $\beta$ -amyloid peptide specifically interacts with and is degraded by insulin degrading enzyme. *FEBS Lett.*, **345**, 33–37 (1994).
  - 38) McDermott, J. R., and Gibson, A. M., Degradation of Alzheimer's  $\beta$ -amyloid protein by human and rat brain peptidases: involvement of insulin-degrading enzyme. *Neurochem. Res.*, **22**, 49–56 (1997).
  - 39) Chesneau, V., Vekrellis, K., Rosner, M. R., and Selkoe, D. J., Purified recombinant insulin-degrading enzyme degrades amyloid  $\beta$ -protein but does not promote its oligomerization. *Biochem. J.*, **351**, 509–516 (2000).
  - 40) Kurochkin, I. V., Amyloidogenic determinant as a substrate recognition motif of insulin-degrading enzyme. *FEBS Lett.*, **427**, 153–156 (1998).
  - 41) Affholter, J. A., Cascieri, M. A., Bayne, M. L., Brange, J., Casaretto, M., and Roth, R. A., Identification of residues in the insulin molecule important for binding to insulin-degrading enzyme. *Biochemistry*, **29**, 7727–7733 (1990).
  - 42) Authier, F., Bergeron, J. J., Ou, W. J., Rachubinski, R. A., Posner, B. I., and Walton, P. A., Degradation of the cleaved leader peptide of thiolase by a peroxisomal proteinase. *Proc. Natl. Acad. Sci. U.S.A.*, **92**, 3859–3863 (1995).
  - 43) Betton, J. M., Sassoon, N., Hofnung, M., and Laurent, M., Degradation versus aggregation of misfolded maltose-binding protein in the periplasm of *Escherichia coli*. *J. Biol. Chem.*, **273**, 8897–8902 (1998).